Journal of Non-Crystalline Solids 538 (2020) 120010

Contents lists available at ScienceDirect

Journal of Non-Crystalline Solids

journal homepage: www.elsevier.com/locate/jnoncrysol

Investigations on nonlinear optical properties of gold nanoparticles doped fluoroborate glasses for optical limiting applications

Abhiram Jagannathan[a,b], R. Rajaramakrishna[a,e,*], K.M. Rajashekara[b,*], Jagannath Gangareddy[c,d], Vinayak Pattar K[b,f], Venugopal Rao S[g], Eraiah B[c], Jagadeesha Angadi V[h], J. Kaewkhao[e], S. Kothan[i]

[a] Department of Post Graduate Studies and Research in Physics, The National College, Jayanagar, Bengaluru 560070, Karnataka, India
[b] Department of Physics, S J C Institute of Technology Chickaballapura-562101, Karnataka, India
[c] Department of Physics, Jnana Bharathi Campus, Bangalore University, Bengaluru, 560056, Karnataka, India
[d] Department of Physics, K S Institute of Technology, Bengaluru, 560109, Karnataka, India
[e] Center of Excellence in Glass Technology and Material Science (CEGM), Rajabhat University, Nakhon Pathom, 73000 Thailand
[f] Jawaharlal Nehru Centre for Advanced Scientific Research, Bengaluru, 560064, Karnataka, India
[g] Advanced Centre of Research in High Energy Materials (ACRHEM), University of Hyderabad, Hyderabad-500046, Telangana, India
[h] Department of physics, P C Jabin science college, Hubballi, 580031, Karnataka, India
[i] Center of Radiation Research and Medical Imaging, Department of Radiologic Technology, Faculty of Associated Medical Sciences, Chiang Mai University, Chiang Mai, 50200, Thailand

ARTICLE INFO

Keywords:
Fluoroborate glasses
Gold nanoparticles
Surface plasmon resonance
Nonlinear optical properties
Optical limiting

ABSTRACT

Gold nanoparticles (NPs) exhibit strong surface plasmon resonance (SPR) in the visible spectral region. Lithium Zinc Calcium Fluoroborate glasses embedded with Au NPs were synthesized by conventional melt quench technique. The gold NPs embedded glasses exhibited dichroic nature. A small kink around 44.61° in the X-ray diffraction (XRD) pattern suggests the presence of Au (2 0 0) in the matrix. High resolution-transmission electron microscopic (HR-TEM) measurements further confirmed the existence of spherical and ellipsoidal Au NPs. Thermogravimetric analysis (TGA) reveals the role of network modifiers in the matrix as the glasses that contained higher concentration of lithium oxide exhibits lower T_g thereby resulting in creation of more non bridging oxides (NBO's). The Z-Scan studies were performed under non-resonant condition (800 nm) to analyze the application of these glasses for optical limiting devices.

Introduction

Glasses are interesting materials for nonlinear optical devices due to their wide range of applications in the field of photonic devices viz., lasers, light emitting diodes (LED's), solar cells, nano photonics, optical data storage and sensors [1]. The color of glass in transmitted region occurs due to various mechanisms such as due to absorption of metal ions or band-edge cut-off, or precipitation of colloids etc. The transition metal ions doped in glasses exhibit absorption bands in visible and infrared regions due to its open valence- shell electronic structure that arises due to 3d-3d electronic transitions [2]. The noble metal nanoparticles (MNPs) exhibit a characteristic feature of surface plasmon resonance (SPR) that occurs due to the collective oscillation of conducting electrons at the surface of dielectric medium. The properties of MNPs are largely depends on the shape, size and their distribution in dielectric host. Generally, the SPR and interband transitions of noble metal clusters partially overlap and as a result when they are excited under the SPR resonant conditions, the electrons in the bands of d and s-p will engage in nonlinear process [1,3]. The small size gold nanoparticles (NPs) have large spectrum of potential applications in various field such as biomedical sensing, cellular imaging, cancer therapy, catalysis, electronics and nonlinear optics [4]. The bright ruby red color produced by the addition of small quantity of gold is attributed the Mie scattering and surface plasmon resonance absorption by metal NPs that are embedded in the glass matrix and it has been reported earlier that, there is a strong enhancement of the third-order nonlinear optical ($\chi^{(3)}$) susceptibility and exhibits reversible saturable absorption (RSA) behavior at higher intensities have potential application for optical limiting devices [5]. The photo stability of Au NPs has led to create tremendous potential usage in photonics especially in optical limiters. Optical

* Corresponding authors.
E-mail address: r.rajaramakrishna@gmail.com (R. Rajaramakrishna).

https://doi.org/10.1016/j.jnoncrysol.2020.120010
Received 24 January 2020; Received in revised form 26 February 2020; Accepted 28 February 2020

limiters play a vital role in protection of sensitive optical devices and human eye from high intense radiations [6,7].

Nonlinear optical (NLO) properties for metal NPs have been studied extensively in SPR condition for MNPs. When photo excitation occurs near to SPR region of Au NPs the optical nonlinearities are enhanced. The Z-Scan setup is sensitive and very conventional for measuring the NLO properties of materials compared to other available techniques and it can estimate real and imaginary part of susceptibility simultaneously along with the sign of nonlinearity [8,9].

Addition of alkali oxide like lithium or sodium to B_2O_3 network results in conversion of trigonal to tetrahedral borates groups upto certain concentrations of alkali content and later depolymerizes the network thereby forming trigonal groups by creating excess of non bridging oxygen(NBO's) in the network, this phenomenon is referred to boron oxide anomaly [10–12]. The NBO's are more polarizable than bridging oxygens as they lead to increase in the refractive index of glasses. It was reported earlier that the addition of alkali, alkaline earth, and aluminum fluorides for durable fluoroberyllate glasses has shown excellent ultraviolet transmission and a small increase in nonlinear refractive index (n_2) which is apt for nonlinear device applications. Materials having a large n_2 and small absorption loss coefficient have potential for optical switching devices, that works in operating wavelength [13].

The preliminary investigations provide us an insight to choose an appropriate matrix pertaining to oxyfluorides in borate glasses which can be doped with gold as it is expected to enhance the nonlinear optical properties of glasses that are apt for optical limiting applications. This work suggests the role of network modifiers in Au doped glasses which tunes the structure and nonlinear optical properties of glasses.

Experimental details

Glasses pertaining to composition (wt%) xLi$_2$O - (35-x)CaF$_2$ - 20ZnO - 45B$_2$O$_3$ - 0.1AuCl$_3$ (x = 15, 20) of 10 gm batch were synthesized by the conventional melt quench technique. The highly pure analytical reagent (AR) grade precursors were used and their respective composition details are provided in the table 1. The batches were heat treated in step process to expel hydrates (at 200 °C for 20 min), chlorides (at 450°C for 20 min) and carbonates (at 650 °C for 45 min). The molten glass was stirred continuously for 15 min at 1050 °C and then quenched on preheated (at 200 °C) brass molds. The prepared glass samples were annealed for 300 °C in order to remove the thermal stresses which are occurred while quenching from high temperature. The prepared glasses are coded as A1, A2 for base glasses and G1, G2 for Au NPs containing glasses.

The observed brown colored glasses (as appeared) that transmit blue color (when exposed to white light) indicates that gold NPs are dissolved in the glass and as a result the glasses exhibited dichroic nature as shown in Fig. 1. The prepared glass samples were well polished for optical and NLO characterizations. Optical absorption data were collected by Perkin-Elmer lambda 75 Ultraviolet-Visible (UV–Vis) spectrometer and NLO properties were evaluated using Z- Scan technique at 800 nm using 150 laser pulses fired at a rate of 80 MHz from Ti: Sapphire Laser. Samples were crushed and grinded into fine powders which were characterized for structural and morphological studies viz., XRD (PAN-Analytical Xpert 3), IR (Perkin-Elmer), TGA (TA instruments SDT Q600) and HR-TEM (JEOL/JEM 2100).

Table 1
Glass compositions and their labels used in the study.

Glass Code	Glass Composition (wt%)
A1	15Li$_2$O-20CaF$_2$-20ZnO-45B$_2$O$_3$
A2	20Li$_2$O-15CaF$_2$-20ZnO-45B$_2$O$_3$
G1	15Li$_2$O-20CaF$_2$-20ZnO-45B$_2$O$_3$-0.1 AuCl$_3$
G2	20Li$_2$O-15CaF$_2$-20ZnO-45B$_2$O$_3$- 0.1 AuCl$_3$

Results and discussions

XRD results

The XRD pattern of all investigated glasses demonstrated broad hump between 20°-40° as shown in Fig. 2 confirms that all the samples are amorphous in nature. For samples G1 and G2 there is a peak at 44.61° indicating the gold NPs are of FCC lattice (2 0 0) [14]. The Miller indices for this peak can be estimated by using Braggs equation, $2d_{(hkl)}sin\theta = n\lambda$, where $\lambda_{Cu} = 0.154nm$, d_{hkl} is the inter planar distance, and for FCC lattice parameter $a = 2r\sqrt{2}$, where r is the atomic radius of gold which is 0.166 nm [15]. The relationship between a and $d_{(hkl)} = \frac{a}{\sqrt{(h^2+k^2+l^2)}}$ results in estimation of interplanar distance between to Au planes which is found to be 0.2347 nm. The average crystallite size d of Au NPs can be estimated using Debye-Scherrer's Formula i.e., $= \frac{0.9\lambda}{\beta\cos 2\theta}$, where β is the FWHM (full width half maximum) of diffraction peak and θ is the Bragg's angle. The average crystallite size was estimated to be more for sample G1 compared to G2 and for G2 it was found to be 23.68 nm which further matched with those estimated from HR-TEM images [14].

Physical properties

Physical Properties of glasses were determined by Archimedes method using toluene as the immersing liquid and other parameters were calculated using the formulae mentioned in reference [16]. Table 2 clearly suggests that incorporation of gold in matrix has reduced the density there by increasing the distance between two boron atoms. The increase in molar volume due to presence of gold NPs draws an indication that Au enhances in creating NBO's that lead to open structure in Li$_2$O-CaF$_2$-ZnO-B$_2$O$_3$ glasses [17]. It is observed that, the density of the glass matrix which contains higher concentration of Li$_2$O less than that of glass contained lower concentration of Li$_2$O, thereby it suggests that incorporation of gold assists alkaline element lithium to create NBO's. It can also be observed that the interionic distance between Au-Au has been more in G2 glass which supports our argument on the role of modifier lithium for G2 glass increases more NBO's which thereby results in enhancement of NLO properties [18].

TGA analysis

The TGA/DTA data of glasses shown in Fig. 3 confirms that the glasses doped with (G1, G2) and without (A1, A2) gold in the matrix results in two different kinds of mechanism. The average single bond enthalpy (E_B) of glasses can be correlated with the T_g. The E_B was estimated for the A1, A2, G1 and G2 using the following equations [19].

$$E_B = \frac{xE_{Li-O} - (35-x)E_{Ca-F} - 20E_{Zn-O} - 45E_{B-O} - 0.1E_{Au-Au}}{100}, \quad (1)$$

Where,

$$E_{Li-O}(Li - O = \frac{341kJ}{mol}),$$
$$E_{Ca-F}(Ca - F = \frac{527kJ}{mol}),$$
$$E_{Zn-O}(Zn - O = \frac{284.1kJ}{mol}),$$
$$E_{B-O}(B - O = \frac{806kJ}{mol}),$$
$$E_{Au-Au}(Au - Au = \frac{221.3kJ}{mol}),$$

are the bond energies of single bonds in the matrix [15]. For glasses pertaining to the matrix A1 and G1 the glass transition temperature (T_g) has increased there by CaF$_2$ involves in creation of bridging oxygens in

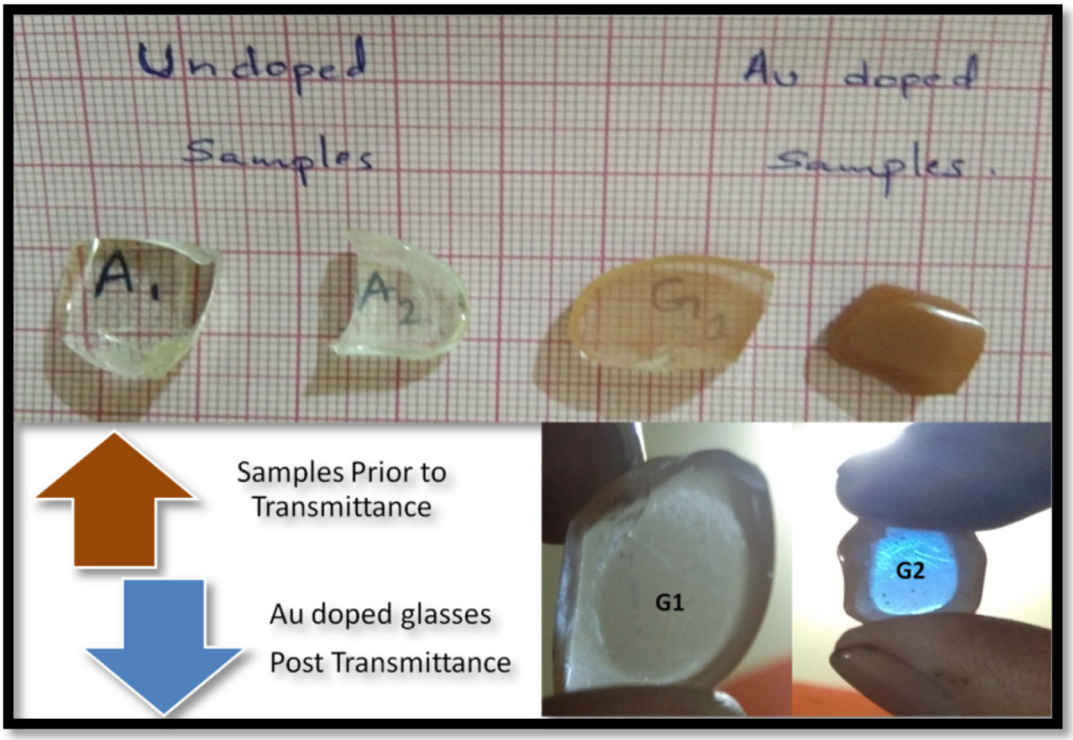

Fig. 1. Dichroic behavior of Au doped Lithium Zinc Calcium fluoroborate glasses (G1 and G2).

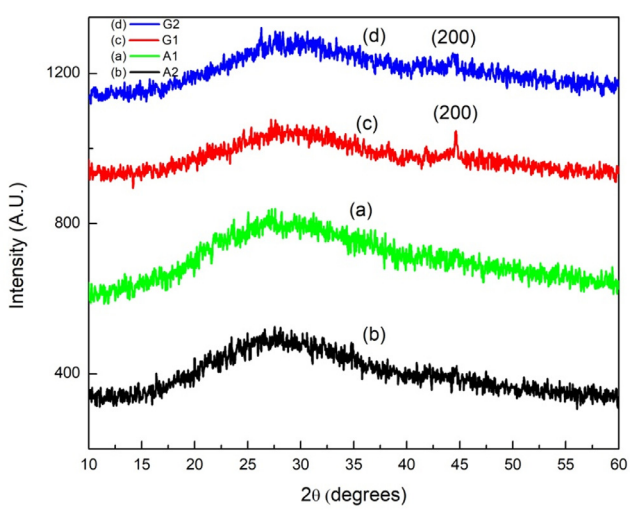

Fig. 2. XRD patterns of A1, A2, G1, and G2 glasses.

the network. As the glass A1 and G1 exhibits bond strength of 576.06 kJ/mol and 576.281 kJ/mol respectively, the increase in single bond strength enthalpy is due to presence of higher concentration of alkaline earth Ca^{2+}or the bond energies of Ca-F around 527 kJ/mol compared to that of Li-O which is 341 kJ/mol. On the contrary, the glass doped with higher concentration of lithium, A2 and G2 exhibits lower Tg which indicates that the dominance of lithium in the network compared to that of calcium fluoride leads in creating more trigonal borate segments for samples A2 and G2 as compared to that in A1 and G1. Thus lithium involves in creating more NBO's in the network [20]. The observation of single bond strength in the matrix of glasses A2 and G2 are 549.72 kJ/mol and 549.94 kJ/mol respectively, it suggests that there is no much difference is bond strength when compared with base glass and doped glass and it can be established from the fact that the alkali modifier Li^{+}in this matrix provides lesser cross linking coordination of oxygen compared to Ca^{2+} which thereby lowers T_g for A2 and G2 glasses [20].

IR studies

The infrared absorbance spectrum shown in Fig. 4(a) confirms the presence of BO_3 and BO_4 structural units of glass as depicted in Table 3. FTIR deconvolution spectra were performed based on [21] using fityk computer software [22]. The spectrum can categorically be divided into three borate segments. First borate band appears around 600–800 cm^{-1} which is attributed to B-O-B bending vibrations where the oxygen atom is linked to one tetrahedral and trigonal group. Second borate segment around 800–1200cm^{-1} confirms the presence of symmetric stretching of tetrahedral BO_4 groups [23] as reported by Doweidar et al. [24] that confirms the presence of distorted $Ca_{1/2}{}^{2+}[BO_{3/2}F]^{-}$ tetrahedral group in the same region which could have lead to formation of oxyfluoride network in the glasses as shown in Eq. (3). The contribution for the formation of oxyfluoride tetrahedral which appears in the same wave number region of tetrahedral borates [25] is partly from modifier CaF_2 and the rest of CaF_2 converts into CaF_4 tetrahedral units [26,27]. The third group between 1200$cm^{-1}$and 1800cm^{-1} confirms the stretching vibrations of B-O in trigonal BO_3 or $[BO_2O]^{-}$ groups [28]. The vibrational modes for the modifying cations like Li^{+}/Ca^{2+} found to be active in the region 400–600 cm^{-1}. The vibration of the OH−, water and B-OH are observed in the region 1700–4000 cm^{-1} [28,29]. There is no signature of Au leading to structural changes, but depending on the lithium concentration structural changes has been observed because the Li^{+}bond disruption energy (Au-O; 223 kJ/mol) compared to Li-O (340.5 kJ/mol). Hence, Li_2O acts as an intermediate in the G2 glass. The Eq. (2) advances in these glasses hence their molar volume is higher than A2 and G2 glasses suggesting loosening in their network formation .The role of CaF_2 helps in creating more bridging oxygen as a result the matrix tightens the network which can be correlated with the increase in T_g [30]. In case of glasses doped with and without gold (A1 and G1 composition), suggests that the Li^{+}plays a role of modifier that creates more bridging oxygens this may be due to presence of higher

Table 2
Optical and physical properties of gold doped Li_2O-CaF_2-ZnO -B_2O_3 glasses.

Optical, Physical and inter-nuclear properties	A1	A2	G1	G2
Density (g/cc) ± 0.02	2.837	2.833	2.830	2.794
Molar Volume unit (cm^3) ± 0.02	23.859	23.041	23.988	23.432
Au ion Concentration (10^{20} atoms/cm^3) ± 0.02	–	–	1.70	1.68
Interionic Distance (10^{-9} m) (± 0.02)	–	–	1.803	1.811
Polaron Radius (Å) ± 0.02	–	–	7.268	7.290
Average B-B distance (Å) ± 0.02	3.302	3.264	3.308	3.282
Glass Transition Temperature (T_g) °C	427.46	420.46	427.30	404.12
Nonlinear Refractive Index- n_2 (10^{-19} m^2/W) ± 0.01	–	–	2.1	4.2
Nonlinear Absorption Coefficients α_2 (cm/GW) ± 0.01	–	–	1.02	1.64
Surface Plasmon Resonance Peak Position (10^{-9} m)	–	–	605.50	579.27
Optical energy bandgap (eV) ± 0.01	3.45	3.29	3.06	2.94
Size of Au nanoparticles (10^{-9} m) (Debye-Scherrer Method)	–	–	36.73	23.68
Size of nano particles (10^{-9} m) (Mie Scattering)	–	–	29.456	29.53

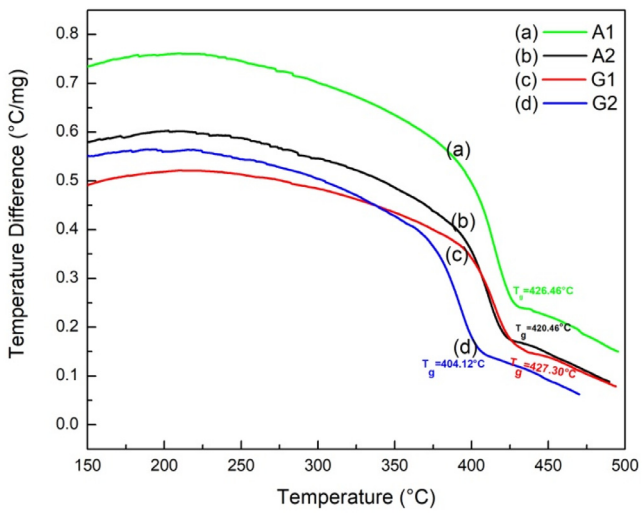

Fig. 3. TGA curve exhibiting glass transition temperature for A1, A2, G1 and G2 glasses.

concentration of modifier alkali element CaF_2 and less Li_2O content which promotes in tighten the network and forming BO_4 as presented in Eq. (4 and 5) hence, there is a decrease in Tg [20] as well as reduces Au which is reflected in its band gap.

$$[BO_{4/2}]^- + [BO_{3/2}] + 0.5O^{2-} \rightarrow 2[BO_{2/2}O]- \quad (2)$$

$$CaF_2 + B_2O_3 \rightarrow 2Ca_{1/2}{}^{2+}[BO_{3/2}F]^- \quad (3)$$

$$2[BO_{3/2}] + O^{2-} \rightarrow 2\ [BO_{4/2}]^- \quad (4)$$

$$Au^+ + e^- \rightarrow Au^0 \quad (5)$$

The structural modification of borates due to calcium can be understood by observing the slight change in the shift in bands towards higher wave number for B-O-B bending vibrations and tetrahedral region in A1 and G1 which leads to reduction in the degree of disorder in the glass network and on the contrary, for A2 and G2 the reverse trend is observed, thereby indicating that the concentration lithium in matrix leads deformer the network in glass [31].

UV–Visible-NIR studies

The samples G1 and G2 exhibit broad shoulders at 604 nm and 578 nm respectively due to surface plasmon resonance [14]. The incorporation of lithium into matrix has reduced more gold and thereby it

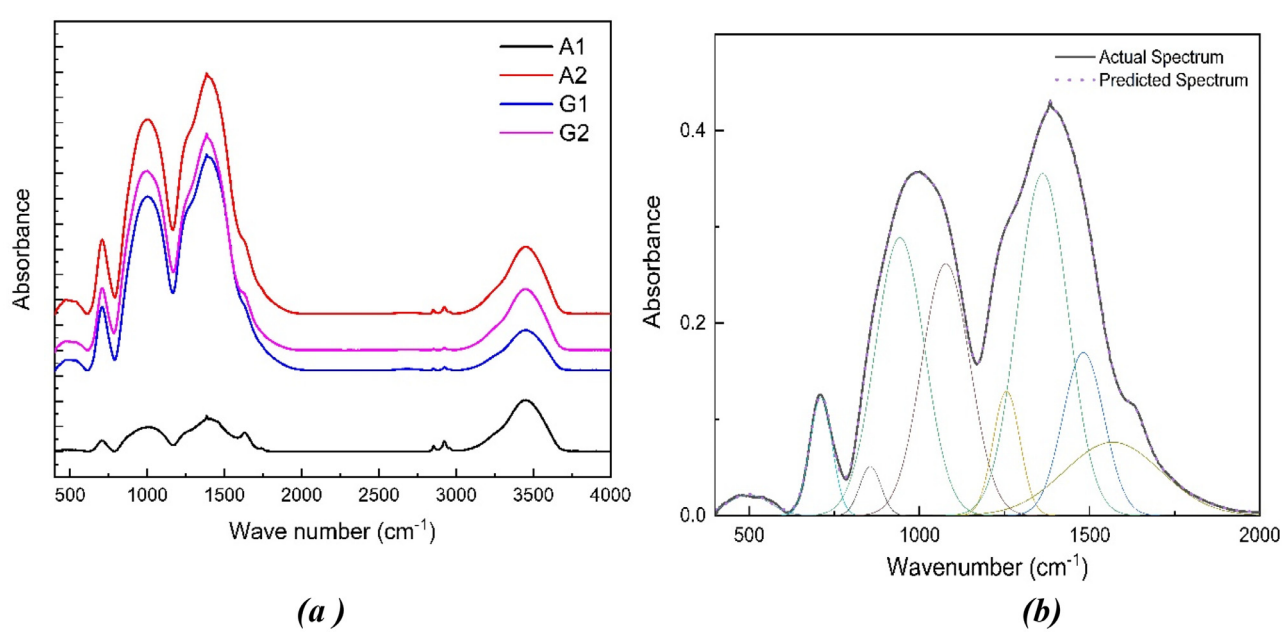

Fig. 4. (a)*:* IR Spectra of A1, A2, G1, and G2 glasses and (b) Deconvoluted Spectra of G2 glass.

Table 3
Structural confirmation of Borate segments in Lithium Zinc Calcium fluoroborate glasses.

Sl. No.	Wave number (cm^{-1})	Spectral Assignments
	400–620	Metallic Vibrations of Li^+, Ca^{2+}, Zn^{2+}
	620–780	B-O-B bending Vibrations (oxygen linkages between trigonal and tetrahedral borate)
	780–1170	Stretching vibration of BO_4 units, Presence of oxyfluoride network
	1170–1700	Stretching vibrations of BO_3 units
	1700–4000	-OH, water and B-OH linkage

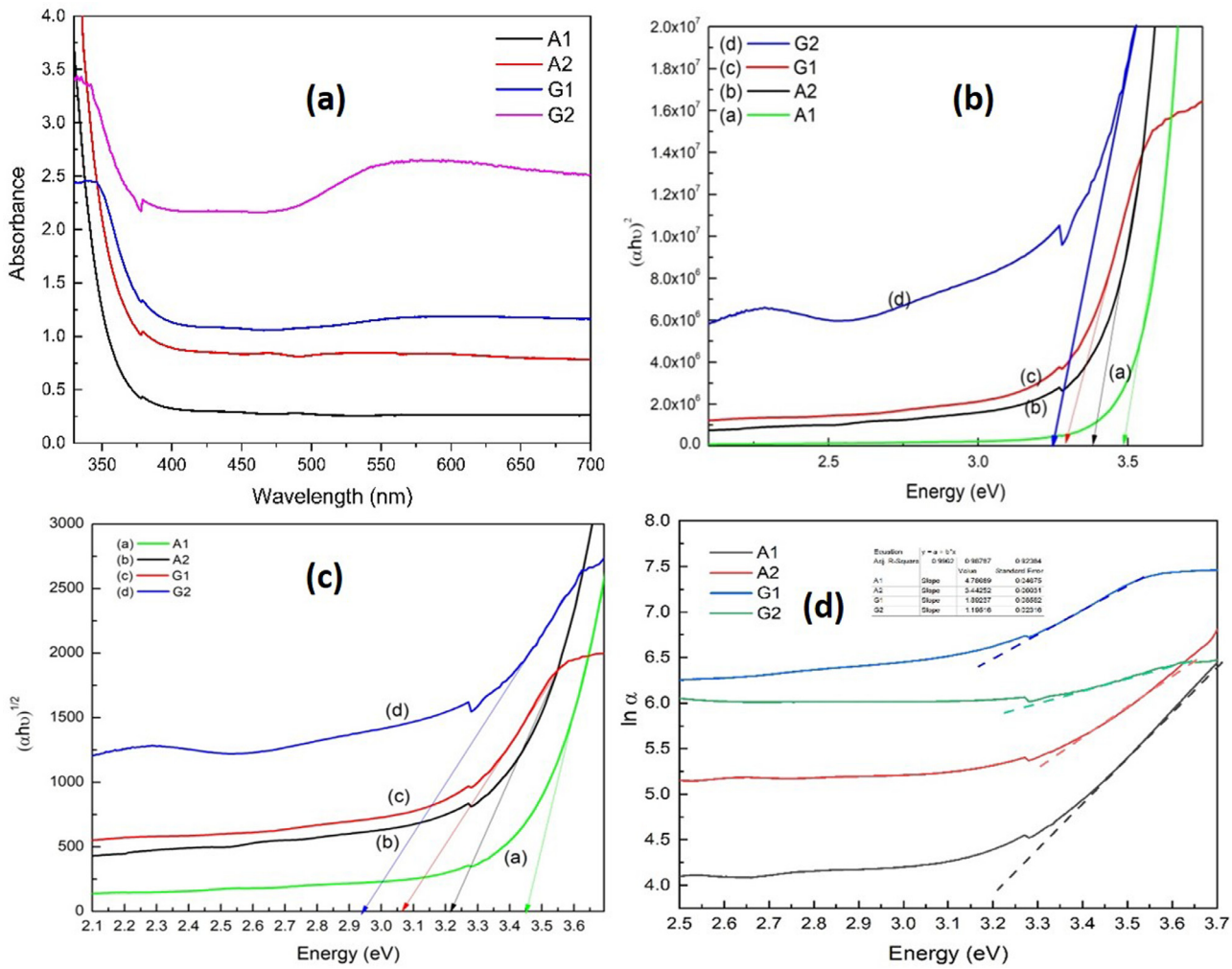

Fig. 5. (a): Absorption profile (b) Direct bandgap (c) Indirect bandgap (d) Urbach Plot for A1, A2, G1, and G2 glasses.

suggests that the probability of reducing $Au^+ \rightarrow Au^0$ is more in G2 compared to G1 which further confirmed from the intensity of absorption profile as shown in Fig. 5(a).

The results also suggest that increasing the concentration of modifying cation like lithium tends to blue shift the band position of Au SPR thereby leading to much comparatively larger size of NPs [32] in G2 samples. When the energy transition occurs between top of the valence band to bottom of the conduction band under the same momentum space, it leads to direct bandgap which can be estimated from the absorption spectra by plotting $(\alpha h\nu)^2$ against energy. Similarly, if the energy transition occurs with different momentum space for energies that are not aligned, which requires and additional energy leads to photon assisted indirect bandgap that is estimated by from the plot $(\alpha h\nu)^{1/2}$ against energy. Both direct and indirect bandgap values are drawn by extrapolating the edge line from the plot [33]. Fig. 5(b) and (c) suggests that the band gap energy reduces for G1 and G2 samples and it also indicates that higher concentration of Li^+ in the matrix promotes more NBO's which can be correlated with the physical properties, TGA and IR results. The bandgap values in series A1 is higher comparatively to that of A2 thereby, the reduction in bandgap is generally due to creation of more non bridging oxygens in the network and in addition to this the incorporation of gold nanoparticles in the matrix has further shifted the optical bandgap to the lower values, this can be well established as there is an increase in molar volume. Further, the strength of disorderness in the network can be interpreted by plotting $ln\alpha$ against energy [33] as shown in Fig. 5(d). The inverse of slope defines Urbach energy (E_u).The Urbach energy for A1 (0.208 eV), A2 (0.290 eV), G1 (0.528 eV) and G2 (0.836 eV) respectively, indicates that there is an increase in Urbach energy with glasses doped with gold which indicates that the probability of NBO's in the network in more compared to that of base glass. The Urbach energy is found to be highest for G2 suggesting that the Au entering into the matrix is able to create more NBO's because the host element has more Li^+ which supports in creating the NBO's in network.

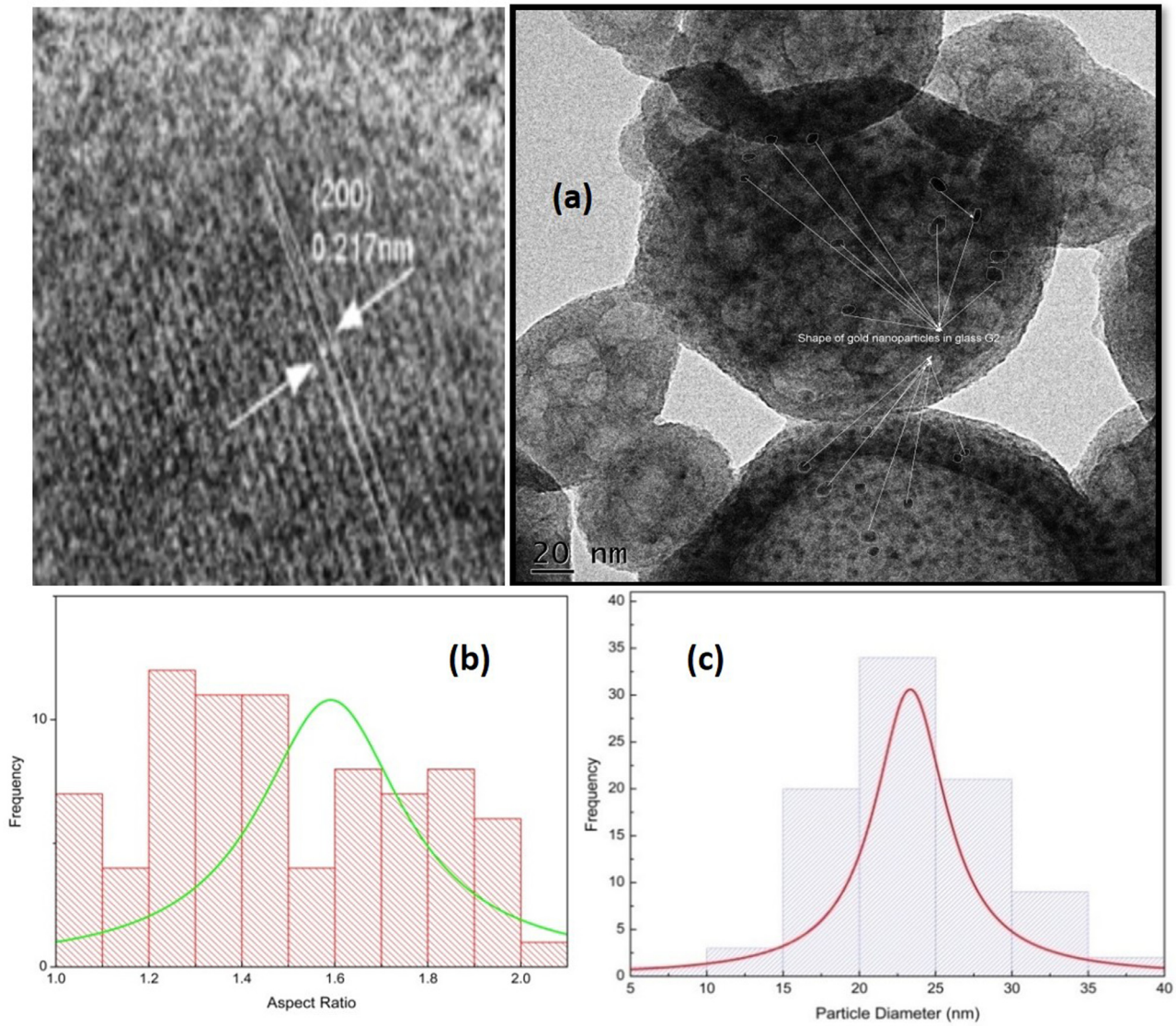

Fig. 6. (a): HR-TEM image confirming uniform distribution of Au NP's in G2 Glass (Inset HR TEM image of 2 nm Au NP's depicts the inter planar distance of Au) (b) Histogram to depict the probability of shapes in Au NPs that are formed in G2 Glass (c) Histogram to depict particle size of Au NPs in G2 Glass.

The size of NPs estimated theoretically by applying Mie theory as mentioned in the reference [32].

$$r = \frac{Av_f}{2\pi c\left(\frac{\Delta\lambda}{\lambda^2_{SPR}}\right)} \tag{6}$$

where, $A = 1.2$, V_f is the Fermi velocity of gold for bulk medium i.e., 13.82×10^5 m/s, c is speed of light in vacuum, $\Delta\lambda$ is FWHM and λ^2_{SPR} is the surface plasmon resonance wavelength. This expression is valid only for spherical nanoparticles. Since our glass exhibits dichroic nature, it can be assumed that there could be a probability of particles to be elliptical with lesser aspect ratio which is closer to 1. If that case is valid, then ellipsoid can be considered and spherical and the apparent sizes of Au NP's were found to be around 30 nm.

Morphological analysis

The morphological features of Au NPs were analyzed using ImageJ software. It was found that the gold NPs have been distributed evenly in the $20Li_2O$-20ZnO-$15CaF_2$-$65B_2O_3$ matrix has as shown in Fig. 6(a) and it also confirms that the spacing between Au NPs in the glass matrix is found to be around 2.0 Å (shown in the inset image), this result are in good agreement with XRD data. It is interesting to note that the shape of NPs has been distributed in form of spherical (when aspect ratio (a/b is 1:1 or 1.0) and ellipsoidal as it approaches higher aspect ratio as shown in Fig. 6(b). The maximum probability on finding the shape in this matrix confirms that the gold NPs have exhibited the shape of ellipsoidal which was found to be in aspect ratio of 3:2 or1.6 thereby, it confirms that the dichroic nature of this glass is due to presence of elliptical Au NPs [14]. The average particle diameter of Au NPs is estimated and shown in histogram in Fig. 6(c). The data suggests that the average particle size is found to be around 23 nm which is correlated with the values those obtained using Debye Scherrer method in XRD.

NLO studies

The NLO experiments were performed at 800 nm obtained using Ti: Sapphire 800 nm laser pulses. In the Z-scan experiment, a lens is used for focusing the laser beam and optically transparent polished sample which moves along the beam axis or the Z-axis through the focal region. At each Z point (i.e., position of the sample), the sample undergoes variable intensity of the laser beam at each position and the transmitted energy was measured using the energy meter placed after the sample. The readings were taken directly to the Z axis lead to open aperture

data (measuring absorption coefficient) and the readings that were taken with help of an aperture lead to closed aperture data (measuring nonlinear refractive index).

The open aperture (OA) and closed aperture (CA) data of Z-scan instruments evaluates nonlinear absorption and refraction properties which vary with respect to intensity of incident beam on the sample along the beam axis.

The OA data was fitted using the equation

$$T_{OA} = \frac{1}{[1 + \alpha_2 L_{eff}][I_{00}/(1 + (Z/Z_0)^2)]} \tag{7}$$

in the above equation, L_{eff} is the effective path length of the sample over the length L, I_{00} is the laser irradiance intensity. The closed aperture data was fitted using the equation

$$T_{CA} = 1 + \frac{4\Delta\varphi_0(Z/Z_0)}{[1 + (Z/Z_0)^2][9 + (Z/Z_0)^2]} \tag{8}$$

where $Z_0$the Rayleigh Range which is often is calculated by the relationship $\frac{\pi\omega_0{}^2}{\lambda}$, where$\omega_0$ is the beam waist and λ is the wavelength of operating laser, φ_0 is the phase difference that is attributed to nonlinear refraction which can be estimated from the curve fitted data, thus the nonlinear refractive index (n_2) was calculated using the expression$\frac{|\Delta\varphi_0|\lambda}{2\pi L_{eff} I_{00}}$ [34]. There was pronounced nonlinearity in the sample G2 compared to G1. Fig. 7(a) data suggests that, as the samples approaches $Z = 0$ or the focal point, intensity gradually decreases i.e., there is a dip in focal region accompanied later by an elevation in focal region, thus leading to positive nonlinear refractive index ($n_2 > 0$) which indicates that the beam is said to exhibit self-focusing nature.

The closed aperture (CA) data reveals that the nonlinear refractive index was found to be higher with increase in concentration of Li_2O since the probability of presence of boron tri oxide is more this may lead to agglomeration of Au NP's or formation of clusters which the nonlinear properties of glasses [30]. The nonlinear refractive indices of these glasses were estimated to be 2.1×10^{-19} m^2/W for G1 and $4.2 \times 10^{-19} m^2/W$ for G2. The OA data shown in Fig. 7(b) clearly demonstrated of valley indicates that the sample exhibits Reverse Saturable Absorption (RSA) which can be arises due inter ($d \rightarrow sp$) and intra band($sp \rightarrow sp$)transitions that occur in Au NPs [34]. The nonlinear absorption coefficient for sample that contained lesser concentration of lithium was 1.02 cm/GW and for the sample that contained more lithium was found to be 1.64 cm/GW. The depth of valley is found to increase with increase in lithium concentration. The role of modifiers in glass is crucial for design of optical limiters which can resist high intense beam. Since these glasses have higher absorption coefficient and lower refractive index, these glasses can be used as optical limiters which can be confirmed from figure of merit [34].

$$F = \frac{2\alpha_2}{n_2}\lambda,$$

$$\textit{Where, } \alpha_2 \textit{ is nonlinear absoprtion co} - \textit{efficient, } n_2 \textit{ is nonlinear refractive index and } \lambda \textit{ is wavelength of operating laser } (800nm) \tag{9}$$

The figure of merit for both the glasses is found to be greater than one, interestingly the glass that contained lesser lithium oxide concentration is more transparent than that of higher concentration of lithium oxide. This may be due to larger nonlinear absorption and larger nonlinear refractive index for the sample G2 might have appeared due to increase in non-bridging oxides in samples [18], whereas comparatively the value of the nonlinear refractive index in sample G1 is found to lower. It can be found that these glasses are not apt for optical switching application and hence these glasses are potential for ultra-fast optical limiters [35]which can abstain high energy laser radiation thereby the material protects optical detectors and human eyes when exposed to laser radiation around this wavelength [7].

Table 4 draws a comparison between various Au NPs doped glasses and the results suggest that, the synthesized Au NP embedded glasses (G1 and G2) exhibits better nonlinear absorption coefficient compared to glasses doped with NZB series, GB-Au and Au NPs doped in monolith glass whereas the glasses NB1, NB2 and NB3, BBS Au-1, BBS Au-2, Au NP in L-8 have shown much better results than our glass, this might be because of the presence of heavy metal oxides in the matrix viz., antimony, bismuth and lead which leads to pronounced nonlinearity [36]. It also suggests that the silicate glasses show better absorption compared to borate glasses, which is quite clear from the results of BBS Au-1, BBS Au-2, Se:0Sn:5Au, 5Se:5Sn:2Au. The result from the data available as per our knowledge in Table 4 clearly suggests that the nonlinearity of glasses depends upon the host matrix and the concentration of dopant.

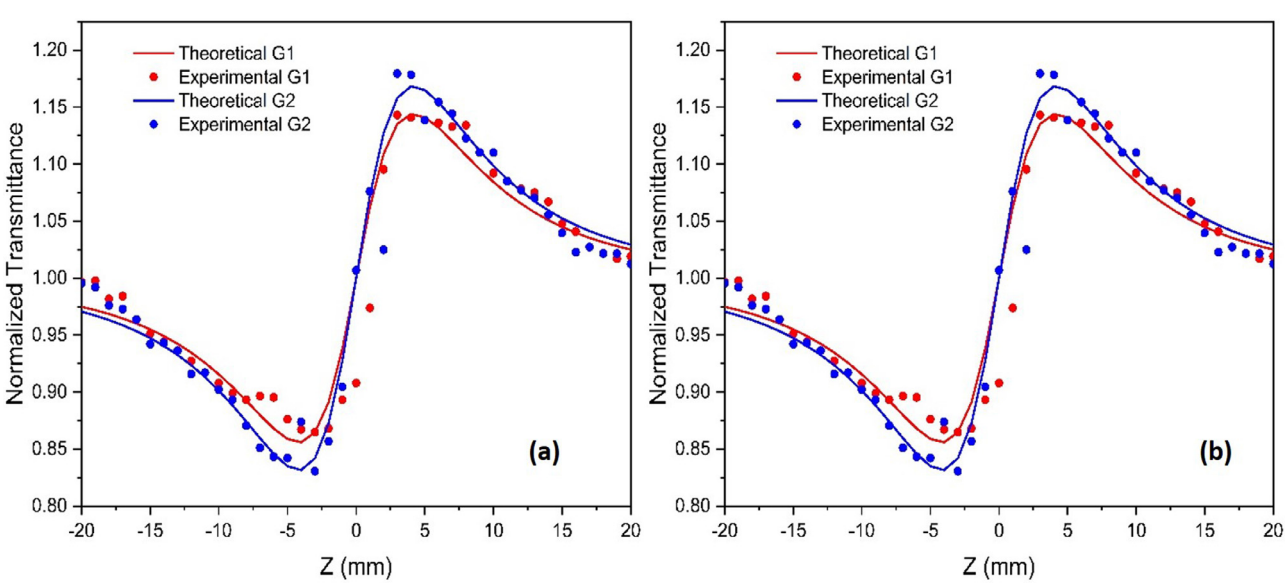

Fig. 7. (a) Closed aperture Z-Scan signature (b) Open aperture Z-scan signature of gold NPs embedded glasses. In above figures the symbols represent the experimental data points while the solid lines indicate the theoretical fits.

Table 4
Comparative study on nonlinear optical behavior of Au nanoparticles doped in various glass systems.

Glasses Studies	Glass System	Nonlinear Refractive Index n_2 (m^2/W)	Nonlinear Absorption Coefficient $\alpha_2(m/W)$
G1 [Present Work]	Borate	$0.21 \times 10^{-18} \pm 0.01$	1.02×10^{-11}
G2[Present Work]	Borate	$0.42 \times 10^{-18} \pm 0.01$	1.64×10^{-11}
Au NP in L1-4 without heat treated, Z-scan studies Performed at 532 nm, 5 ns pulses [37]	Borate	–	6.4×10^{-12}
Au NP in L1-8 without heat treated, Z-scan studies Performed at 532 nm, 5 ns pulses [37]	Borate	–	1.89×10^{-11}
NB-1, Z-scan studies Performed at 532 nm, fs pulses [34]	Borate	-2.84×10^{-16}	1.82×10^{-11}
NB-2, Z-scan studies Performed at 532 nm, fs pulses [34]	Borate	-3.22×10^{-16}	2.02×10^{-11}
NB-3, Z-scan studies Performed at 532 nm, fs pulses [34]	Borate	-3.91×10^{-16}	2.41×10^{-11}
NBS-10 Z-scan studies Performed at 800 nm, 150fs pulses [35]	Antimony Borate	0.21×10^{-18}	0.14×10^{-11}
NBS-20 Z-scan studies Performed at 800 nm, 150fs pulses[35]	Antimony Borate	0.51×10^{-18}	0.46×10^{-11}
NBS-30 Z-scan studies Performed at 800 nm, 150fs pulses[35]	Antimony Borate	0.87×10^{-18}	0.82×10^{-11}
GB-Au, Z-scan studies Performed at 500 nm [38]	Germanium Bismutate	0.18×10^{-19}	0.09×10^{-11}
1NZB, Z-scan studies Performed at 800 nm,150 fs and 80 MHz [33]	Borate	-1.2×10^{-16}	5.2×10^{-14}
2NZB, Z-scan studies Performed at 800 nm, 150 fs and 80 MHz [33]	Borate	-1.9×10^{-16}	4.6×10^{-14}
3NZB, Z-scan studies Performed at 800 nm, 150 fs and 80 MHz [32]	Borate	-2.8×10^{-16}	8.1×10^{-14}
0Sn-0Se-5Au, Z-scan studies Performed at 532 nm Continuous wave [32]	Silicate	–	2.06×10^{-10}
5Sn-5Se-2Au, Z-scan studies Performed at 532 nm, Continuous wave [32]	Silicate	–	2.33×10^{-10}
BBS- Au1, Z-scan studies Performed at 800 nm, 56 MHz and 200fs [39]	Bismuth borate silicate	4.65×10^{-16}	7.4×10^{-11}
BBS- Au2, Z-scan studies Performed at 800 nm 56 MHz and 200fs [39]	Bismuth borate silicate	3.13×10^{-16}	5.1×10^{-11}
Au ions in GIL49 Performed at 800 nm, 1 kHz repetition rate and 25 fs pulses [34]	Silicate	–	7.72×10^{-11}
Au ions in BK7 Performed at 800 nm, 1 kHz repetition rate and 25 fs pulses [40]	Silicate	–	16.3×10^{-11}
Au ion in Glass B Performed at 800 nm, 1 kHz repetition rate and 25 fs pulses [40]	Silicate	–	5.25×10^{-11}
Au Nanoparticle doped monolith glass at 800 nm, 20 kHz repetition rate and 196 fs pulses [41]	Silicate	3×10^{-20}	-6.5×10^{-14}
Au Nanoparticles embedded silica glass performed at 720 nm fs pulses [42]	Silicate	1.74×10^{-18}	5.72×10^{-12}

Conclusions

The role of Li_2O and CaF_2 due to presence of gold NPs in the fluoroborate glasses is reported. FTIR deconvolution suggests that there is a probability of formation of $[BO_{3/2}F]$ from CaF_2 thereby confirming the presence of oxyfluoride network in the matrix. The dopant gold plays a supporting role in enhancing NBO's in the network. Since the concentration of Li_2O is higher in G2 compared to G1, the probability of NBOs is found to be higher which can be correlated as the optical bandgap values were red shifted, thereby the samples doped with gold with more concentration of lithium content (G2) has resulted in better the nonlinear refractive index and nonlinear absorption coefficient.

Author contributions

J. Abhiram and dr. R.R.K. designed the overall research, Z-Scan measurement was characterized by J.Abhiram and G.J in Advanced center of Research in High Energy Materials (ACRHEM) with the help of Prof. S.V. R. The overall work was discussed with Prof J. K, Prof. B.E, dr. J. Angadi, Prof S Kothan and Prof K. M. R to interpret results; K. V helped to characterize XRD, IR and UV . J. Abhiram drafted the manuscript.

CRediT authorship contribution statement

Abhiram Jagannathan: Data curation, Formal analysis, Investigation, Methodology, Software, Validation, Writing - original draft, Writing - review & editing. **R. Rajaramakrishna:** Conceptualization, Funding acquisition, Methodology, Project administration, Resources, Supervision, Validation, Writing - review & editing. **K.M. Rajashekara:** Supervision. **Jagannath Gangareddy:** Data curation, Formal analysis, Software, Writing - review & editing. **Vinayak Pattar K:** Data curation. **Venugopal Rao S:** Project administration, Supervision, Writing - review & editing. **Eraiah B:** Methodology, Supervision. **Jagadeesha Angadi V:** Supervision. **J. Kaewkhao:** Conceptualization, Funding acquisition, Resources, Supervision. **S. Kothan:** Funding acquisition, Supervision.

Declaration of competing interest

The authors declare that they have no known competing financial interests or personal relationships that could have appeared to influence the work reported in this paper.

Acknowledgements

The authors AJ and RRK are indebted to Dr. A.H. Rama Rao, President, NES of Karnataka, Prof. S.N. Nagaraja Reddy, Secretary, NES of Karnataka Dr. B.R. Parineetha, Principal, The National College Jayanagar and Dr. N.G. Pramod, Department of Physics (P.G.), The National College Jayanagar (NCJ) for facilitating glass synthesis. This research was partially supported by Chiang Mai University. The author (s) thank SAIF-Sophisticated Analytical Instrument Facility, Karnataka University, Dharwad, India for providing TGA experimental facility. The author(s) thank STIC facility, CUSAT KOCHI for HRTEM.

References

[1] B. Karmakar, R. Klaus, A. Stepanov, Glass Nanocomposites, Elsevier, 2016, 10.1016/C2014-0-02375-1.
[2] A. Edgar, Optical properties of glasses, Opt. Prop. Condens. Matter Appl. John Wiley & Sons, Ltd, 2006, pp. 159–196 10.1002/0470021942.ch8.
[3] B. Karthikeyan, J. Thomas, R. Kesavamoorthy, Optical limiting with off-resonant excitations in Ag nanocomposite glasses: a z-scan study, J. Non-Cryst. Solids. 353 (2007) 1346–1349 10.1016/j.jnoncrysol.2006.11.025.
[4] V. Amendola, R. Pilot, M. Frasconi, O.M. Maragò, M.A. Iatì, Surface plasmon resonance in gold nanoparticles: a review, J. Phys. Condens. Matter. 29 (2017) 203002 10.1088/1361-648X/aa60f3.
[5] R. Rajaramakrishna, C. Saiyasombat, R.V. Anavekar, H. Jain, Structure and nonlinear optical studies of Au nanoparticles embedded in lead lanthanum borate glass, J. Non-Cryst. Solids 406 (2014) 107–110 10.1016/j.jnoncrysol.2014.09.052.

[6] R. Philip, G.R. Kumar, N. Sandhyarani, T. Pradeep, Picosecond optical nonlinearity in monolayer-protected gold, silver, and gold-silver alloy nanoclusters, Phys. Rev. B. 62 (2000) 13160–13166 10.1103/PhysRevB.62.13160.

[7] R. Udayabhaskar, B. Karthikeyan, P. Sreekanth, R. Philip, Enhanced multi-phonon Raman scattering and nonlinear optical power limiting in ZnO:Au nanostructures, RSC Adv. 5 (2015) 13590–13597 10.1039/C4RA11204K.

[8] M. Sheik-bahae, A.A. Said, E.W.V. Stryland, High-sensitivity, single-beam n_2 measurements, Opt. Lett. 14 (1989) 955–957 10.1364/OL.14.000955.

[9] C. Li, Nonlinear Optics: Principles and Applications, Springer, Singapore, 2017 10.1007/978-981-10-1488-8.

[10] E James Shelby, Introduction to Glass Science and Technology, 2nd Edition, The Royal Society of Chemistry, UK, 2005.

[11] K.J. Rao, Structural Chemistry of Glasses, 1st Edition, Elsevier, New York, 2002.

[12] N.J. Kreidl, A dedication to krogh-moe: his contribution to the understanding of borate glasses, in: L.D. Pye, V.D. Fréchette, N.J. Kreidl (Eds.), Borate Glas. Struct. Prop. Appl. Springer, US, Boston, MA, 1978, pp. 1–10 10.1007/978-1-4684-3357-9_1.

[13] M.J. Weber, Optical properties of glasses, Mater. Sci. Technol. American Cancer Society, 2006, 10.1002/9783527603978.mst0101.

[14] T. Som, B. Karmakar, Surface plasmon resonance and enhanced fluorescence application of single-step synthesized elliptical nano gold-embedded antimony glass dichroic nanocomposites, Plasmonics 5 (2010) 149–159 10.1007/s11468-010-9129-8.

[15] J.A. Dean, N.A. Lange (Eds.), Lange's Handbook of Chemistry, McGraw-Hill, New York, 1973.

[16] S. Kaewjaeng, S. Kothan, W. Chaiphaksa, N. Chanthima, R. Rajaramakrishna, H.J. Kim, J. Kaewkhao, High transparency La2O3-CaO-B2O3-SiO2 glass for diagnosis x-rays shielding material application, Radiat. Phys. Chem. 160 (2019) 41–47 10.1016/j.radphyschem.2019.03.018.

[17] M.S. Gaafar, N.S.A. El-Aal, O.W. Gerges, G. El-Amir, Elastic properties and structural studies on some zinc-borate glasses derived from ultrasonic, ft-ir and X-ray techniques, J. Alloys Compd 475 (2009) 535–542 10.1016/j.jallcom.2008.07.114.

[18] B. Shanmugavelu, V.V. Ravi Kanth Kumar, R. Kuladeep, D. Narayana Rao, Third order nonlinear optical properties of bismuth zinc borate glasses, J. Appl. Phys. 114 (2013) 243103 10.1063/1.4858422.

[19] N. Kaur, A. Khanna, M. Gónzález-Barriuso, F. González, B. Chen, Effects of Al3+, W6+, Nb5+ and Pb2+ on the structure and properties of borotellurite glasses, J. Non-Cryst. Solids 429 (2015) 153–163 10.1016/j.jnoncrysol.2015.09.005.

[20] N.B. Pimentel, V.R. Mastelaro, J.-.C. M'Peko, S.W. Martin, S.S. Rojas, J.E. De Souza, Structural and electrical characterization of glasses in the Li2O–CaO–B2O3 system, J. Non-Cryst. Solids 499 (2018) 272–277 10.1016/j.jnoncrysol.2018.07.024.

[21] A.M. Abdelghany, The elusory role of low level doping transition metals in lead silicate glasses, Silicon 2 (2010) 179–184 10.1007/s12633-010-9053-8.

[22] M. Wojdyr, Fityk: a general-purpose peak fitting program, J. Appl. Crystallogr. 43 (2010) 1126–1128 10.1107/S0021889810030499.

[23] C. Gautam, A.K. Yadav, A.K. Singh, A review on infrared spectroscopy of borate glasses with effects of different additives, Int. Sch. Res. Not. 428497 (2012) 1–17 10.5402/2012/428497.

[24] H. Doweidar, G. El-Damrawi, M. Abdelghany, Structure and properties of CaF2–B2O3 glasses, J. Mater. Sci. 47 (2012) 4028–4035 10.1007/s10853-012-6256-y.

[25] A.M. Abdelghany, H.A. ElBatal, R.M. Ramadan, The effect of Li2O and LiF on structural properties of cobalt doped borate glasses, J. King Saud Univ. - Sci. 29 (2017) 510–516 10.1016/j.jksus.2016.09.003.

[26] A.M. Abdelghany, H.A. ElBatal, Optical and μ-FTIR mapping: a new approach for structural evaluation of V2O5-lithium fluoroborate glasses, Mater. Des. 89 (2016) 568–572 10.1016/j.matdes.2015.09.159.

[27] A.M. Abdelghany, H.A. ElBatal, F.M. EzzElDin, Influence of CuO content on the structure of lithium fluoroborate glasses: spectral and gamma irradiation studies, spectrochim, Acta. A. Mol. Biomol. Spectrosc. 149 (2015) 788–792 10.1016/j.saa.2015.04.105.

[28] S. Ibrahim, F.H. ElBatal, A.M. Abdelghany, Optical character enrichment of NdF3 – doped lithium fluoroborate glasses, J. Non-Cryst. Solids. 453 (2016) 16–22 10.1016/j.jnoncrysol.2016.09.017.

[29] A.M. Ibrahim, A.H. Hammad, A.M. Abdelghany, G.O. Rabie, Mixed alkali effect and samarium ions effectiveness on the structural, optical and non-linear optical properties of borate glass, J. Non-Cryst. Solids. 495 (2018) 67–74 10.1016/j.jnoncrysol.2018.05.015.

[30] Y.D. Yiannopoulos, G.D. Chryssikos, E.I. Kamitsos, Structure and properties of alkaline earth borate glasses, Phys. Chem. Glas. 42 (2001) 164–172.

[31] S.V.G.V.A. Prasad, G. Sahaya Baskaran, N. Veeraiah, Spectroscopic, magnetic and dielectric investigations of BaO–Ga2O3–P2O5 glasses doped by Cu ions, Phys. Status Solidi A. 202 (2005) 2812–2828 10.1002/pssa.200521131.

[32] J. Abhiram, R. Rajaramakrishna, Y. Ruangtaweep, J. Kaewkhao, Effect of SnO2 and SeO2 in non-linear optical properties of Au nanoparticle doped self striking red ruby glasses, Thai J. Nanosci. Nanotechnol. 4 (2019) 12–19.

[33] S.B. Kolavekar, N.H. Ayachit, G. Jagannath, K. NagaKrishnakanth, S. Venugopal Rao, Optical, structural and Near-IR NLO properties of gold nanoparticles doped sodium zinc borate glasses, Opt. Mater. 83 (2018) 34–42 10.1016/j.optmat.2018.05.083.

[34] J. Gangareddy, E. Bheemaiah, V. Gandhiraj, J.T. James, J.K. Jose, K. Katturi Naga, V.R. Soma, Nonlinear optical studies of sodium borate glasses embedded with gold nanoparticles, Appl. Phys. B. 124 (2018) 205 10.1007/s00340-018-7074-y.

[35] G. Jagannath, B. Eraiah, A. Gaddam, H. Fernandes, D. Brazete, K. Jayanthi, K.N. Krishnakanth, S. Venugopal Rao, J.M.F. Ferreira, K. Annapurna, A.R. Allu, Structural and femtosecond third-order nonlinear optical properties of sodium borate oxide glasses: effect of antimony, J. Phys. Chem. C. 123 (2019) 5591–5602 10.1021/acs.jpcc.8b09466.

[36] I.A. Denisov, A.G. Selivanov, K.V. Yumashev, A.V. Anan'ev, L.V. Maksimov, N.V. Ovcharenko, V.N. Bogdanov, A.A. Lipovskii, A.N. Vlasova, Nonlinearity of refractive index in glasses based on heavy metal oxides with different lead and tellurium contents, J. Appl. Spectrosc. 74 (2007) 866–871 10.1007/s10812-007-0134-4.

[37] R. Rajaramakrishna, S. Karuthedath, R.V. Anavekar, H. Jain, Nonlinear optical studies of lead lanthanum borate glass doped with Au nanoparticles, J. Non-Cryst. Solids. 358 (2012) 1667–1672 10.1016/j.jnoncrysol.2012.04.031.

[38] J.M.P. Almeida, D.S. da Silva, L.R.P. Kassab, S.C. Zilio, C.R. Mendonça, L.D. Boni, Ultrafast third-order optical nonlinearities of heavy metal oxide glasses containing gold nanoparticles, Opt. Mater. 36 (2014) 829–832 10.1016/j.optmat.2013.12.012.

[39] F. Chen, S. Dai, T. Xu, X. Shen, C. Lin, Q. Nie, C. Liu, J. Heo, Surface-plasmon enhanced ultrafast third-order optical nonlinearities in ellipsoidal gold nanoparticles embedded bismuthate glasses, Chem. Phys. Lett. 514 (2011) 79–82 10.1016/j.cplett.2011.08.011.

[40] R. Ahmad, M. Shahid Rafique, A. Ahmed, A. Ajami, P. Nekvindova, B. Svecova, S. Bashir, S. Iqbal, Femtosecond laser induced two-photon absorption in Au-ion embedded glasses, Laser Part. Beams 37 (2019) 61–66 10.1017/S026303461900020X.

[41] H. Gao, W. Xiang, X. Ma, L. Ma, Y. Huang, H. Ni, X. Shi, G. Chen, X. Liang, Sol-gel synthesis and third-order optical nonlinearity of Au nanoparticles doped monolithic glass, Gold Bull 48 (2015) 153–159 10.1007/s13404-015-0173-1.

[42] X. Zhang, W. Luo, L.-.J. Wang, W. Jiang, Third-order nonlinear optical vitreous material derived from mesoporous silica incorporated with Au nanoparticles, J Mater Chem C 2 (2014) 6966–6970 10.1039/C4TC00856A.